Theor Chim Acta (1988) 73: 27–42

Theoretica Chimica Acta

Structure and properties of nonclassical polymers*

IV. The effect of long-range Coulomb interaction on the elementary excitation spectrum

Christo I. Ivanov, Nikolai Tyutyulkov**, Gottfried Olbrich, H. Barentzen, and Oscar E. Polansky**

Max-Planck-Institut für Strahlenchemie, Stiftstrasse 34-36, D-4330 Mülheim a.d. Ruhr, Federal Republic of Germany

(Received March 27; revised and accepted July 20, 1987)

Utilizing an extended Hubbard-type Hamiltonian which incorporates both nearest-neighbour Coulomb repulsion and exchange interactions, we have studied the energy dispersion of the lowest elementary excitation from the ferromagnetically aligned state of quasi one-dimensional alternant hydrocarbon networks. It was found that the main effect of the long range Coulomb interaction may be thought of as a renormalization (screening) of the on-site Hubbard integral. This implies an enhancement of the kinetic exchange term and impairs the stability of the ferromagnetic state towards single spin inversions. However, for physically relevant values of the parameters entering the model Hamiltonian, the collective spin excitation represents a magnon, whose energy band lies above the reference value pertaining to the magnetically saturated configuration.

Key words: Organic magnetism — Alternant polymers — Magnon — Effective Heisenberg exchange

1. Introduction

In two previous papers [1, 2] the authors dealt with a special class of polymers exhibiting a system of conjugation to which no Kekulé formula [3] can be

* Dedicated to Prof. Dr. Adolf Neckel on the occasion of his 60th birthday

** *Permanent address*: Bulgarian Academy of Sciences, Institute of Organic Chemistry, 113 Sofia, Bulgaria

attributed. For the latter reason such organic systems with conjugated π electron networks were termed alternant nonclassical polymers (ANCP).

In general, an alternant hydrocarbon is characterized by a partitioning of its atoms into two disjoint subsets of n^* starred and n° unstarred atoms, such that $n^* + n^\circ = n$, where n denotes the total number of atoms in the system. A particularly interesting class of alternant hydrocarbons is comprised by conjugated networks with $n^* \neq n^\circ$, see, e.g. polymers II, IV, V and VI of [2].

Several theoretical investigations on the ground state spin multiplicity of finite hydrocarbon oligomeres have been carried out recently. Utilizing configuration interaction calculations (CI) for small alternant molecules (biallyl, triallyl, etc.) based on the Hubbard and Pariser-Parr-Pople (PPP) models and a degenerate perturbation cluster expansion approach for the Hubbard model Klein et al. [4] showed that the ground state spin amounts to

$$S = |n^* - n^\circ|/2,$$

a conjecture made earlier by Ovchinnikov [5]. In a related work based on the PPP Hamiltonian Koutecky et al. [6] furnished additional theoretical support for the existence of hydrocarbon molecules with high-spin ground state configuration.

In 1983 Teki et al. [7] succeeded in detecting by ESR spectroscopy an aromatic hydrocarbon phenylenebis ((diphenylmethylen-3-yl)methylene) with a nonet spin multiplicity ($S = 4$) in the electronic ground state. The magnetic alignment of the π electrons at the bridge sites of the tetradiphenylcarbene is further stabilized by the ferromagnetic exchange interaction between these π electrons and the localized nonbonding electrons at the bridge sites. However, the existence of high (macroscopic) spin ($S \approx N$) ground state configurations in extended hydrocarbon networks (polymers) remains an important challenge both for theorists and for the experimental community.

In [1] and [2] the band structure of a series of ANCP's was studied by taking into account electron correlation within the AMO (Alternant Molecular Orbitals) version of the extended Hartree-Fock method. All investigated polymers exhibit the same characteristic band scheme comprising full BMO (Bonding Molecular Orbitals) bands, empty ABMO (Antibonding Molecular Orbitals) bands and an infinitely narrow NBMO (Nonbonding Molecular Orbitals) band. The occurrence of latter is the most conspicuous feature of the band pattern of the alternant non-classical polymers.

In [1] an attempt has been made to draw some conclusions on the energy dependence upon the total spin S_z component, which is determined by the spin configuration in the NBMO band. Although the calculations of [1] shed some light on the 'energy' behaviour with respect to spin reversion in the NBMO band the physical relevance of the matrix elements of the Hamiltonian displayed in this work (cf. Table 1 and Fig. 2 in [1]) is rather limited. Strictly speaking, the matrix elements displayed in Table 1 do not depend merely on the number of inverted spins p but also on the specific configuration $\{k_{i_1}, k_{i_2}, \ldots, k_{i_p}\}$ of Bloch

states ($k_i \in 1BZ$) to which up-spins are assigned. The problem parallels the calculations by Durand et al. [8] who showed that the diagonal matrix elements decreased drastically in value with increasing alternation in the spin distribution.

To remedy the aforementioned difficulty we take in the present paper a rather different approach to study the stability of the saturated ferromagnetic state. Thus proceeding from a fully aligned NBMO band we consider the spectrum of the elementary excitations in dependence of the physical parameters entering the single band NBMO Hamiltonian.

The paper is organized as follows. In Sect. 2 we introduce the Hamiltonian incorporating all relevant Coulomb and exchange interactions. Section 3 deals with the spectrum of the low-lying elementary magnetic excitations and some final comments and conclusions are presented in Sect. 4.

2. The elementary excitation spectrum

The infinite degeneracy in the NBMO band of ANCP's within Hückel MO theory is a consequence of the topological structure of their π electron networks. This is mathematically reflected by the Coulson–Rushbrooke theorem [9] based on the equivalence of the Coulomb integrals at the different sites. However, in a real polymer the σ-core and the fully occupied BMO bands will inevitably cause a widening of the NBMO band. Different substituents will have a similar effect towards removing the band degeneracy. A calculation carried out in [2] shows, however, that the splitting remains small being of order of magnitude $w = 10^{-1}$ eV. Bearing in mind that for a tight-binding band the band width w is connected to the resonance (hopping) integral β by: $w = -2z\beta$, with z the number of nearest-neighbour atoms, one realizes that this implies an effective resonance integral β_{NBMO} which might be of comparable size or even smaller than the exchange interaction integral in the NBMO band. Since magnetic order is known to arise from a nonzero exchange interaction [10, 11] the competition of the nearest-neighbour Coulomb exchange J_{NBMO} and β_{NBMO} is of crucial importance for the type of magnetic correlation. To avoid cumbersome notation we drop in the following the subscript NBMO and introduce the band Hamiltonian in the Wannier representation

$$H = \sum_{\sigma} \sum_{m,n} \beta_{mn} a^{+}_{m\sigma} a_{n\sigma} + \tfrac{1}{2} \sum_{\sigma,\sigma'} \sum_{m,n} U(n-m) a^{+}_{m\sigma} a^{+}_{n\sigma'} a_{n\sigma'} a_{m\sigma}$$
$$+ \tfrac{1}{2} \sum_{\sigma,\sigma'} \sum_{m \neq n} J(n-m) a^{+}_{m\sigma} a^{+}_{n\sigma'} a_{m\sigma'} a_{n\sigma}, \tag{2.1}$$

where $a^{+}_{n\sigma}$ ($a_{n\sigma}$) is the creation (annihilation) operator for an electron at the lattice site (monomeric unit) R_n and β_{mn} are the corresponding Coulomb ($m = n$) and resonance ($n \neq m$) one-electron integrals. The hopping matrix element β_{mn}, $m \neq n$, reflects the electron transfer between states at the mth and nth unit site (monomer). The last two terms in (2.1) describe the e-e interaction with $U(n-m)$ the two-center Coulomb integral and $J(n-m)$ its exchange counterpart. For the

one-electron part of H we shall adopt the tight-binding (Hückel) approximation

$$\beta_{mn} = \begin{cases} \alpha & \text{for } m = n \\ \beta & \text{for } m, n \text{ nearest neighbours} \\ 0 & \text{elsewhere.} \end{cases} \tag{2.2}$$

Now, before we pass to the Bloch representation by means of the Fourier transform

$$a^+_{n\sigma} = N^{-1/2} \sum_k \exp(-ikR_n) a^+_{k\sigma} \tag{2.3}$$

it is expedient to introduce the electron-hole (e-h) operators $\rho^+_k(q)$ by

$$\rho^+_k(q) = a^+_k{\uparrow} a_{k+q}{\downarrow}. \tag{2.4}$$

Since $a^+_{k\sigma}$ ($a_{k\sigma}$) creates (annihilates) an electron in the $|k\sigma>$ state, the operators (2.4) refer to a pairing of a spin-up electron in the state $|k>$ with a spin-down hole in the state $|k+q>$ such that the total quasimomentum of the pair is $\hbar q$.

By virtue of the fact that the Hamiltonian (2.1) conserves the number of spin-up (spin-down) electrons, the number density operators N_σ, $\sigma = \alpha, \beta$, are good quantum numbers, i.e. they are constants of motion

$$[N_\sigma, H]_- = 0 \tag{2.5}$$

with

$$N_\sigma = \sum_n a^+_{n\sigma} a_{n\sigma} = \sum_k a^+_{k\sigma} a_{k\sigma}. \tag{2.6}$$

In view of this we introduce now the subspace X_M of the complete Hilbert space as the subspace spanned by the simultaneous eigenvectors of H and N_α for a fixed eigenvalue, M, of N_α. This implies that for any vector $|\psi_M> \in X_M$ the condition is met: $S_z|\psi_M> = \hbar(M - N/2)|\psi_M>$. Then in X_M the Hamiltonian (2.1) can be expressed in terms of the e-h operators (2.4) only

$$H_M = E_0 + \sum_{k,k'} \sum_q [M^{-1}\omega_k(q)\delta_{kk'} - \Omega_{k-k'}(q)] \rho^+_k(q) \rho_{k'}(q)$$

$$+ \tfrac{1}{2} \sum_q \tilde{U}(q) \sum_{i=1}^{2} \Gamma^+_i(q) \Gamma_i(q), \tag{2.7}$$

where

$$\omega_k(q) = U_0 + \sum_{n \neq 0} J(n) + \varepsilon_k(q) \tag{2.8}$$

with $U_0 = U(n=0)$ the on-site Coulomb repulsion. The e-h energies $\varepsilon_k(q)$ are given by

$$\varepsilon_k(q) = \varepsilon_k - \varepsilon_{k+q}, \tag{2.9}$$

where the one-particle Bloch energies ε_k are

$$\varepsilon_k = \beta \sum_{<n,0>} \cos(kR_n), \tag{2.10}$$

with $\langle n, 0\rangle$ indicating summation over the nearest neighbours of a fixed site (e.g. $R_1 = 0$), which in the one-dimensional case reduces to

$$\varepsilon_k = 2\beta \cos(ka), \tag{2.11}$$

a standing for the lattice spacing. The quantity $\Omega_{k-k'}(q)$ reads

$$\Omega_{k-k'}(q) = U(k-k') + J(q), \tag{2.12}$$

where $U(k)$ and $J(q)$ are the Fourier transforms of the two-electron Coulomb and exchange integrals, respectively (cf. Eq. (2.1))

$$U(k) = N^{-1} \sum_n U(n) \exp[-ikR_n], \tag{2.13a}$$

$$J(q) = N^{-1} \sum_{n \neq 0} J(n) \exp[-iqR_n]. \tag{2.13b}$$

The last term in Eq. (2.7) describes the interactions between different e-h pairs which is easily seen from the form of the operators $\Gamma_i(q)$, $i = 1, 2$

$$\Gamma_1^+(q) = M^{-1} \sum_{k,k'} \rho_{k'}^+(k+q)\rho_{k'}(k), \tag{2.14a}$$

$$\Gamma_2^+(q) = M^{-1} \sum_{k,k'} \rho_{k'}^+(k+q)\rho_{k'+q}(k). \tag{2.14b}$$

Finally $\bar{U}(k)$ reads (cf. Eqs. (2.13))

$$\bar{U}(k) = U(k) - J(k) \tag{2.15}$$

and E_0 is defined by

$$E_0 = \alpha_N + \tfrac{1}{2} \sum_{m,n} [U(n-m) - J(n-m)]. \tag{2.16}$$

Our goal now is to investigate the energetic stability of the state ferromagnetically aligned

$$|\psi_0> = \prod_{k \in 1BZ} a_{k\downarrow}^+ |\text{vac}>, \tag{2.17}$$

with respect to elementary excitations within the NBMO band. Then the quantity E_0 is immediately revealed as the eigenvalue of H corresponding to the ferromagnetic state (2.17) which now plays the role of a new vacuum state. Since we are interested in the spectrum of the elementary excitations ($S_z = -\hbar[N/2 - 1]$) we confine in the following to the dynamics in the subspace $X_{M=1}$. Due to the fact that the pair interaction term of (2.7), cf. also Eqs. (2.14), annihilates states with one reverted spin H_1 takes the following simple form

$$H_1 = E_0 + \sum_{k,k'} \sum_q [\omega_k(q)\delta_{kk'} - \Omega_{k-k'}(q)]\rho_k^+(q)\rho_{k'}(q). \tag{2.18}$$

By virtue of the hermiticity of the matrix

$$W_{kk'}(q) = \omega_k(q)\delta_{kk'} - \Omega_{k-k'}(q) \tag{2.19}$$

H_1 is easily diagonalized by means of the unitary transformation $U(q)$, with matrix elements $u_{kp}(q)$, leading to the collective excitation

$$|\varphi_p(q)> = R_p^+(q)|\psi_0>, \tag{2.20}$$

with

$$R_p^+(q) = \sum_k u_{qp}(q)\rho_k^+(q). \tag{2.21}$$

The wave functions $u_{kp}(q)$, referring to the internal structure of the elementary excitations, and the corresponding energy spectrum are determined by the following eigenvalue equation

$$[\omega_k(q) - E_p(q)]u_{kp}(q) = \sum_{k'} \Omega_{k-k'}(q)u_{k'p}(q), \tag{2.22}$$

where the quantities $\omega_k(q)$ and $\Omega_k(q)$ were defined by Eqs. (2.8) and (2.12), respectively. Eq. (2.22) yields N different solutions for the energy eigenvalue $E_p(q)$ and N^2 solutions for the wave functions $u_{kp}(q)$, $p = 1, 2, \ldots N$, $k \in 1\mathrm{BZ}$.

3. The eigenvalue equation for the collective mode

A detailed study of the elementary magnetic excitation spectrum shows [12] that it consists of a quasicontinuum (of N − 1 energy eigenvalues) and an isolated solution $E_1(q)$ lying below the bottom of the continuum. Hence, in the study of the energetic favourability of the excited states with respect to the fully aligned band it is sufficient to restrict the considerations to the lowest band of collective excitations.

To make Eq. (2.22) amenable to a relatively simple numerical treatment, instead of the general Hamiltonian (2.1) (see also Eqs. (2.7) and (2.18)) we utilize in the present work an extended Hubbard-type Hamiltonian. To this end we introduce some simplifications which, however, do not impair the physical essence of the Hamiltonian. As in the conventional Hubbard model [13, 14] we consider the on-site e-e repulsion U_0, thus maintaining the competition between the interaction U_0, tending towards covalent configurations, and the hopping integral β, which tends to destroy the single-site occupation. However, our model improves upon the Hubbard approximation by taking into account nearest-neighbour Coulomb repulsion integrals U_1 and exchange interaction matrix elements J, the latter competing with the kinetic term β in favour of ferromagnetic correlation. Thus we obtain the following Schrödinger equation for the unknown wave functions u_{kp} and the corresponding band energy E_p

$$[\omega_k(q) - E_p(q)]u_{kp}(q) = (U_0 + 2J\cos qa)N^{-1}\sum_{k'} u_{k'p}(q) + 2U_1 N^{-1}\sum_{k'} \cos[(k-k')a]u_{k'p}(q), \tag{3.1}$$

where the pair energies $\omega_k(q)$ are given by

$$\omega_k(q) = U_0 + 2J + 2\beta \sin(qa/2)\sin(ka + qa/2). \tag{3.2}$$

Since $E_1(q)$ lies far below the continuum of pair energies, $\omega_k(q)$ (see Fig. 7 of [12]), none of the terms $[\omega_k(q)-E_1(q)]$ vanish for $k\in 1\mathrm{BZ}$. Thus, division of Eq. (3.1) by the factor $[\omega_k(q)-E_1(q)]$ and subsequent integration over k, $-\pi< ka\leq\pi$, yields

$$\sqrt{x^2-16\beta^2\sin^2(qa/2)}=U_0+2J\cos qa+U_1L(q)[x+\sqrt{x^2-16\beta^2\sin^2(qa/2)}]. \tag{3.3}$$

Here the unknown function $L(q)$ has been introduced by

$$L(q)=\frac{\sum_k \sin(ka+qa/2)u_{k1}(q)}{2\beta\sum_k \sin(qa/2)u_{k1}(q)}, \tag{3.4}$$

and x is related to the energy eigenvalue E_1 through

$$E_1(q)=x(q)+U_0+2J. \tag{3.5}$$

Fortunately, no explicit knowledge of the wave functions $u_{k1}(q)$ appearing in $L(q)$ is necessary in order to solve Eq. (3.3). This is easily realized by inserting Eq. (3.2) into the Schrödinger equation (3.1) and integrating the latter over k, $-\pi<ka\leq\pi$. One obtains

$$E_1(q)=4[J+2\beta^2L(q)]\sin^2(qa/2), \tag{3.6}$$

which implies immediately $E_1(q=0)=0$. Therefore we can concentrate on the solution of the eigenvalue problem for $q\neq 0$, where $L(q)$ is well defined, see Eq. (3.4). Eliminating $L(q)$ from Eqs. (3.3) and (3.6) we finally arrive at the following identity for the unknown function $x(\omega)$, $\omega=qa$,

$$\sqrt{x^2-f^2(\omega)}\,[f^2(\omega)-2U_1x-2U_1g(\omega)]=2U_1[x^2+g(\omega)x]+g(\omega)f^2(\omega), \tag{3.7}$$

which holds for all $\omega\neq 0$ and $-\pi<\omega\leq\pi$. Here the following abbreviations have been introduced

$$f(\omega)=4\beta\sin(\omega/2) \tag{3.8}$$

and

$$g(\omega)=U_0+2J\cos\omega. \tag{3.9}$$

The algebraic Eq. (3.7) has been solved numerically for a fixed value of the Hubbard parameter $U_0=10$ eV, while the nearest-neighbour Coulomb integral was varied within the range 0–5 eV. For every given value of U_1 several solutions for $E_1(\omega;U_1)$ have been calculated, corresponding to different pairs of values of the resonance integral β and the exchange interaction J, respectively. To facilitate the overview of the plots exhibited in Sect. 4, the different (β,J)-pairs were enumerated and are displayed in Table 1. The same numbers, as those assigned to the six (β,J)-choices of Table 1, have been used to mark the band energy $E_1(\omega;U_1=\text{const.})$.

Table 1. Enumerated (β, J)-pairs (values in eV). $|\beta|$ is the hopping parameter and J the exchange integral

No.	1	2	3	4	5	6
$\|\beta\|$	0.5	0.2	0.2	0.5	1.0	0.6
J	0.1	0.1	0.2	0.001	0.1	0.1

4. Numerical results and discussion

The numerical solution of Eq. (3.7) reveals that the dispersion curve $E_1(\omega)$, $-\pi < \omega \leq \pi$, maintains its qualitative behaviour with increasing values of the nearest-neighbour Coulomb repulsion U_1. For the sake of illustration (Fig. 1) we have plotted the energy $E_1(\omega)$ of the lowest excitation band for three different values of U_1: 0.5, 3 and 5 eV.

The enumeration of the different curves corresponds to the order of the (β, J)-parameter-pairs as displayed in Table 1. The band energy $E_1(\omega)$ is an even function of ω, with $E_1(0) = 0$, and attains its extreme value (maximum or minimum) at the boundary of the Brillouin zone: $\omega = \pi$. $E(\pi) > 0$ implies that the elementary excitation is placed energetically higher than the ordered ferromagnetic state, represented graphically by the horizontal line $E = 0$. In turn $E_1(\pi) < 0$ entails destabilization of the magnetically saturated state with respect to single spin inversions in the NBMO band. Due to assessments carried out in previous work [13] the ANCP's are characterized by a nearest-neighbour exchange interaction J ranging from 0.1 to 0.2 eV, while the next-to-nearest-neighbour exchange term is one or two orders of magnitude smaller than J. Therefore, in our calculations we have restricted the variation of J to the physically significant region $J \leq 0.2$ eV.

Since the quantity $E_1(\pi)$ provides a measure for the energetic favourability of the lowest elementary excitation, and hence for the stability of the ferromagnetically aligned state $|\psi_0>$ toward spin inversion, we considered it worthwhile to study the dependence of $E_1(\pi)$ on the nearest-neighbour repulsion parameter U_1. The interrelation $E_1(\pi)$ versus U_1 has been plotted in Fig. 2 for all six (β, J)-pairs of Table 1, with U_1 ranging from 0 to 5 eV.

It is evident from Fig. 2 that in all cases $E_1(\pi)$ decreases monotonously with increasing values of U_1. In the cases (1)–(5) no qualitative changes occur, in the sense that $E_1(\pi)$ maintains its sign for all values of U_1. However, in the case (6), $|\beta| = 0.6$ ev and $J = 0.1$ eV, $E_1(\pi)$ undergoes a dramatic variation with increasing U_1-values. While the excitation energy $E_1(\pi)$ remains positive in the interval $U_1 < 2.85$ eV, at the point $U_1 = 2.85$ eV the elementary excitation state and the saturated magnetic state $|\psi_0>$ become accidentally degenerate. For values greater than the critical value $U_1 = 2.85$ eV the collective excitation energy $E_1(\pi)$ decreases below the horizontal line $E = 0$, i.e. the ferromagnetically aligned state is destabilized by single spin inversions in the NBMO band.

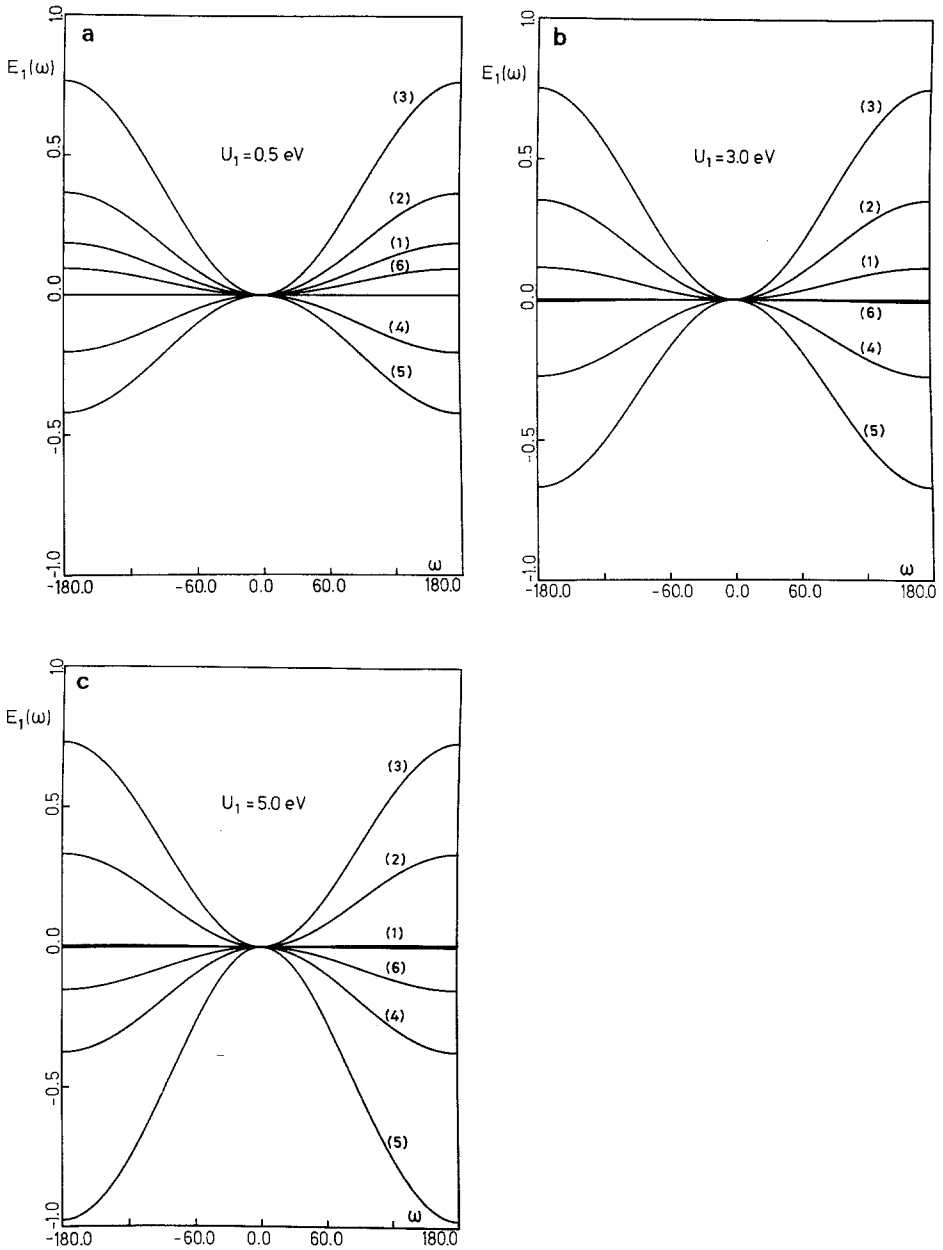

Fig. 1 a–c. Energy dispersion of the lowest elementary excitation band. **a** $U_1 = 0.5$ eV; **b** $U_1 = 3.0$ eV; **c** $U_1 = 5.0$ eV. The curves (1)–(6) correspond to different (β, J)-pairs of values of the resonance and exchange integral, respectively, as given in Table 1

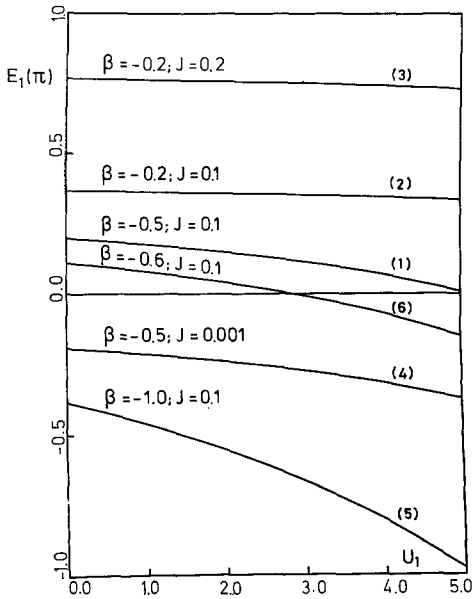

Fig. 2. U_1-dependence of the extremal value of the excitation band energy $E(\pi)$ for different values of the resonance integral β and the exchange interaction J. U_1 ranges between 0 and 5 eV

Comparison of plots (2) and (3), or (1) and (4), shows that for a fixed value of the resonance integral β the energy $E_1(\pi)$ increases nearly proportionally to J. This effect is to be anticipated on general grounds, since according to the theory of magnetism [10, 11] J tends to a ferromagnetic alignment of the electron spins.

The qualitative differences in the behaviour of the extremal value $E_1(\pi)$ with U_1 may be entirely attributed to the variation of the resonance integral β. For small β-values, $|\beta| \leq 0.2$ eV, see curves (2) and (3), $E_1(\pi)$ drops linearly with U_1, the slope being about $-7 \cdot 10^{-3}$. However, for larger values of $|\beta|$ (0.5 to 1.0 eV) the quantity $E_1(\pi)$ begins to diminish faster than linearly, see plots (1) and (4)-(6). Thus in the case (5), where $|\beta| = 1$ eV, the (average) slope equals -0.12 which is more than a factor of 10^2 larger than the slope of curves (2) and (3).

The sequence of the plots (2), (1), (6) and (5) illustrates the decrease of $E_1(\pi)$ with β for a fixed value of the exchange integral J. This effect is accounted for by the fact that the effective electron mass m_{eff} is inversely proportional to the width $w = -2\beta$ of the NBMO band. Or, paraphrasingly, the mobility of the electrons in the NBMO band rises linearly with β and tends to destroy the single-site occupation (Ising configurations) in the polymer chain.

Curves (4) and (6) visualize the crucial role of the competition between the exchange integral J and the hopping parameter $|\beta|$. Although in the latter case enhancement of the electron mobility is to be expected (due to the larger value of $|\beta| = 0.6$ eV), the corresponding $E_1(\pi)$-curve lies above that pertaining to case (4). For $U_1 < 2.85$ eV the single spin inversions in case (6) become energetically disadvantageous compared to the fully aligned state $|\psi_0>$, see horizontal line $E = 0$. This is attributed to the sizeable ferromagnetic correlations within the

NBMO band, originating from the relatively large value of J in case (6), $J = 0.1$ eV, which is greater by a factor of 10^2 than the corresponding value of J in case (4).

Thus the numerical results lead us to the conclusion that the long-range Coulomb interaction lowers the energy of the collective excitations and thus brings about a relative impairment of the stability of the ferromagnetically aligned state with respect to spin inversion in the localized band of the ANCP's.

To form a picture of the quantitative impact of the nearest-neighbour Coulomb interaction U_1 on the effective Heisenberg exchange interaction we introduce at this stage the quantity $\tilde{U}_1$

$$\tilde{U}_1(\omega) = U_0 + 2J + L^{-1}(q), \tag{4.1}$$

where $L(q)$ is defined by Eq. (3.4). This now enables us to rewrite Eq. (3.6) in the following form

$$E_1(\omega) = 4J^{\text{eff}}(\omega) \sin^2(\omega/2), \tag{4.2}$$

where the Heisenberg exchange interaction reads

$$J^{\text{eff}}(\omega) = J - \frac{2\beta^2}{U - \tilde{U}_1(\omega) + 2J\cos\omega}. \tag{4.3}$$

In this way the effect of the long-range Coulomb interaction can be studied on the behaviour of the quantity $\tilde{U}_1(\omega)$, which had been plotted in Fig. 3.

To visualize the variation of $\tilde{U}_1(\omega)$ with U_1 we present here three different plots: *a*) $U_1 = 0.5$ eV, *b*) $U_1 = 3$ eV and *c*) $U_1 = 5$ eV. The marks on the curves for a fixed U_1-value coincide with the (β, J)-pair-enumeration introduced in Table 1. Fig. 3 shows that $\tilde{U}_1(\omega)$ is an even function of ω and its value at the origin $\tilde{U}_1(0)$ is equal to the parameter U_1 itself. The function $\tilde{U}_1(\omega)$ drops monotonously within the interval $0 \leq \omega \leq \pi$ thus reaching its minimum at the boundary of the Brillouin zone.

To illustrate the deviation of $\tilde{U}_1(\omega)$ from the nearest-neighbour repulsion integral U_1 (Eqs. (4.1) and (4.3)), we have exhibited in Fig. 4 the plot $\tilde{U}_1(\pi)$ versus U_1 for $U_1 \leq 5$ eV and different values of the β and J integrals (see Table 1).

To facilitate the discussion we have depicted, in addition, the linear function $f(U_1) = U_1$ by a dashed line. The plots in Fig. 4 reveal a very insensitive variation of $\tilde{U}_1(\pi)$ with J. Thus the curves (2) and (3), which are characterized by the same value $|\beta| = 0.2$ eV and different values $J = 0.1$ and 0.2 eV, respectively, virtually coincide within the scale chosen (according to the numerical calculation the plot (2) lies $2.5\ 10^{-3}$ eV higher than (3)). The same is true of curves (4) and (1), where $|\beta| = 0.5$ eV while the exchange integrals differ by a factor 10^2, being 0.001 and 0.1 eV, respectively.

Next we consider the behaviour of $\tilde{U}_1(\pi)$ for fixed values of the parameter β. Figure 4 shows a linear variation of $\tilde{U}_1(\pi)$ with U_1 for small values of the resonance integral ($|\beta| \leq 0.2$ eV), see curves (2) and (3), whereas for larger values

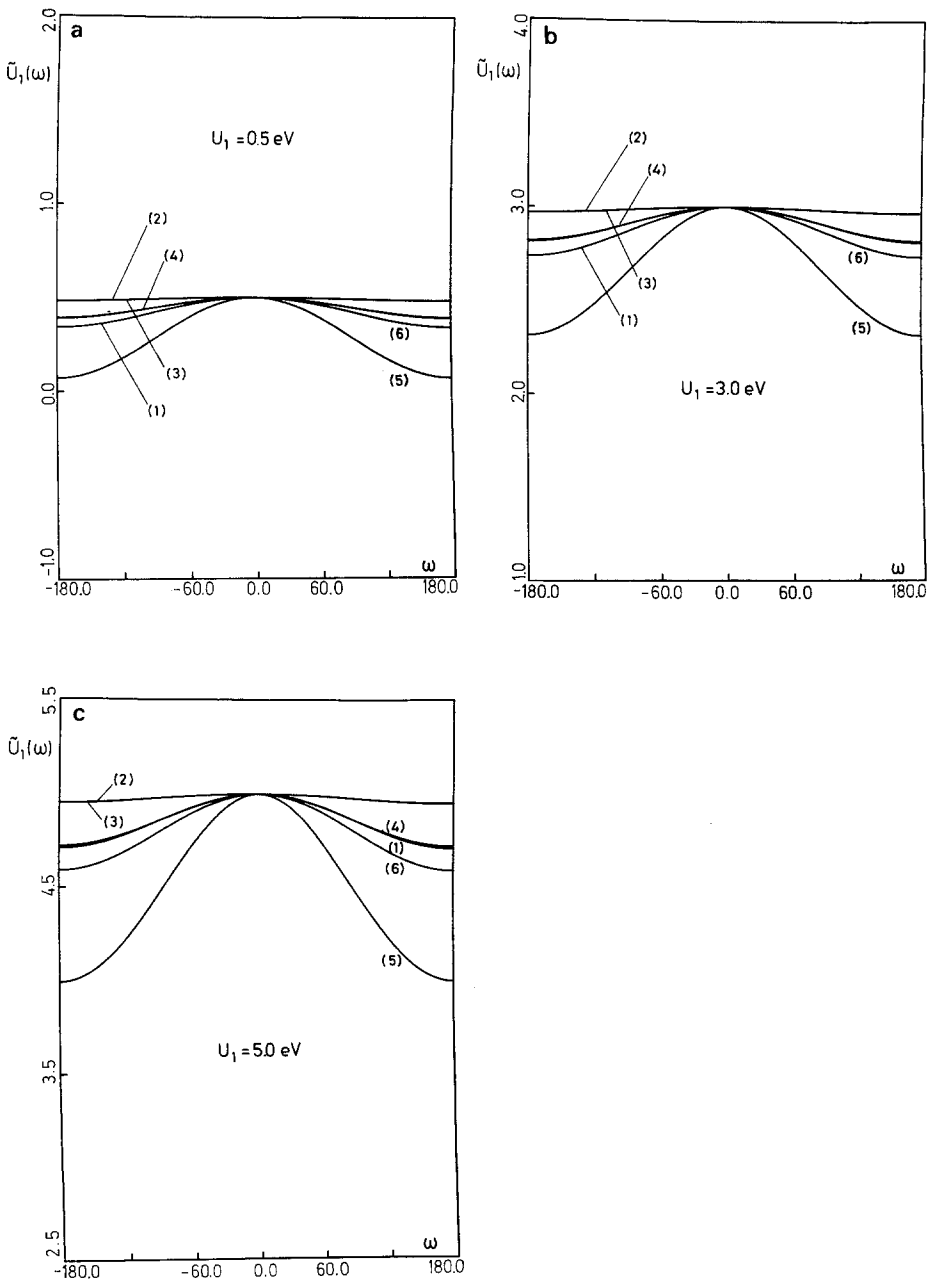

Fig. 3 a–c. Behaviour of the function $\tilde{U}_1(\omega)$ for **a** $U_1 = 0.5$ eV; **b** $U_1 = 3.0$ eV; **c** $U_1 = 5.0$ eV. The marks on the different curves pertain to the different (β, J)-pairs of Table 1

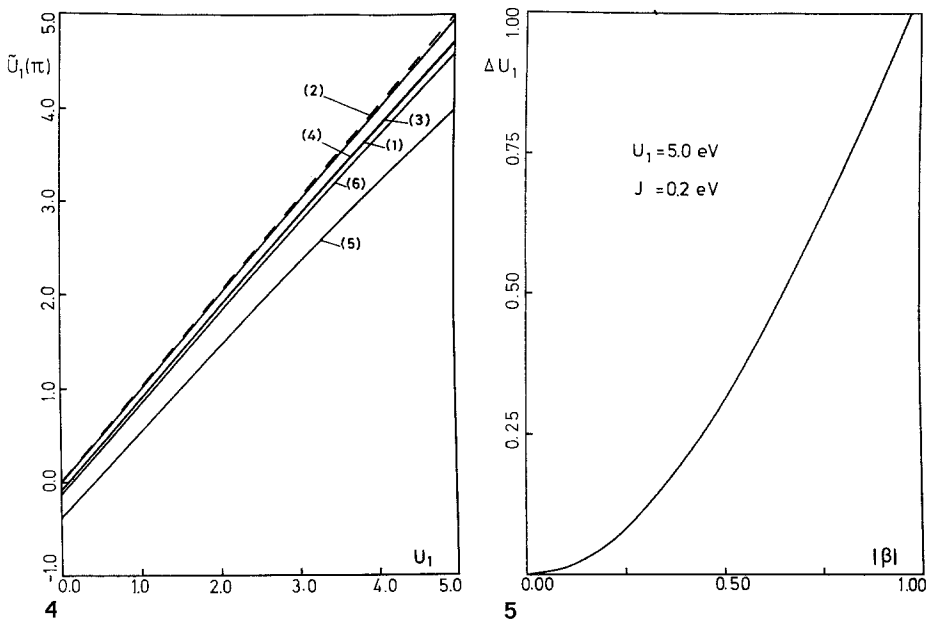

Fig. 4. Graphical representation of the deviation of $\tilde{U}_1(\pi)$ from the nearest-neighbour Coulomb integral U_1: $0 \leq U_1 \leq 5$ eV. The auxiliary function $f(U_1) = U_1$ is depicted by a *dashed line.* The enumeration of the curves is in accordance with Table 1

Fig. 5. Variation of the deviation $\Delta U_1 = U_1 - \tilde{U}_1(\pi)$ with increasing values of the resonance parameter $|\beta|$ for $U_1 = 5.0$ eV and $J = 0.2$ eV

of $|\beta|$, see e.g. plots (6) and (5), $\tilde{U}_1(\pi)$ increases slower than linearly with rising values of U_1. The slope of the curves decreases immaterially with $|\beta|$, thus dropping from 0.99 to 0.87 while $|\beta|$ increases from 0.2 to 1 eV. This indicates a very slow variation of the deviation $\Delta U_1 = [U_1 - \tilde{U}_1(\pi)]$ with U_1. Thus, the most relevant information gained from Fig. 4 consists in the strong dependence of the deviation ΔU_1 on the value of the resonance integral β. The calculation shows that ΔU_1 rises slightly faster than quadratically while the parameter $|\beta|$ increases from 0 to 1 eV. This behaviour is illustrated in Fig. 5 for the following fixed values of the remaining parameters: $U_1 = 5$ eV, $J = 0.2$ eV.

To conclude, we present an attempt at fitting an analytical expression to the exact numerical solutions $E_1(\omega)$ of Eq. (3.7), see also Fig. 1. To this end, we try the following ansatz for the quantity (4.1)

$$\tilde{U}_1(\omega) = a + b \cos \omega \tag{4.4}$$

and determine the coefficients a and b of the above conjecture by means of its values at $\omega = 0$ and at the boundary $\omega = \pi$ of the Brillouin zone. This yields

$$a = [U_1 + \tilde{U}_1(\pi)]/2, \qquad b = [U_1 - \tilde{U}_1(\pi)]/2, \tag{4.5}$$

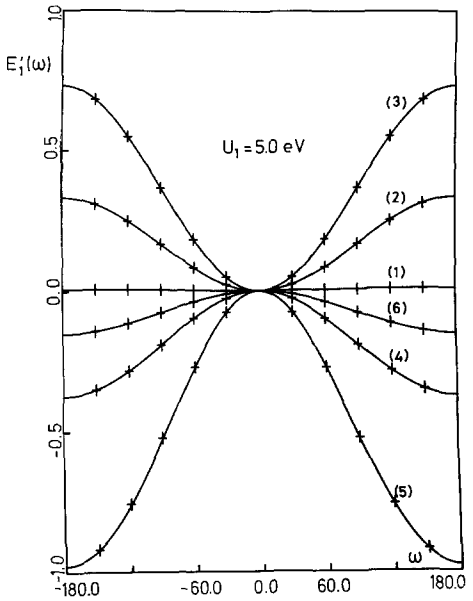

Fig. 6. Graphical representation of the conjecture $E_1'(\omega)$, see Eq. (4.6), for the lowest excitation band for $U_1 = 5.0$ eV and different choices for the (β, J)-pairs, according to Table 1. Crosses (+) represent corresponding numerical values

leading to the following explicit expression for the excitation band energy

$$E_1'(\omega) = 4\left[J - \frac{2\beta^2}{U_0 - a + (2J - b)\cos\omega}\right]\sin^2(\omega/2). \tag{4.6}$$

The prime at E has been used to distinguish between the guessed curve $E_1'(\omega)$ and the exact relation (4.2).

To elucidate the accuracy of the tentative dispersion relation (4.6), in Fig. 6 we have presented the E_1'-plots for $U_1 = 5$ eV and for all (β, J)-parameter sets of Table 1.

By way of comparison, we have marked by crosses the corresponding numerical solutions obtained from Eq. (3.7). Fig. 6 reveals a striking agreement between the suggested dispersion relation (4.6) and the previous numerical results, see also Fig. 1.

The shortcoming of the ansatz (4.4) is the fact that the quantity $\tilde{U}_1(\pi)$, entering expressions (4.5), is an implicit function of the energy $E_1(\omega)$ and hence cannot be determined without recourse to the solution of Eq. (3.7). However, by reference to Fig. 3 it follows that for small values of the resonance integral, $|\beta| \leq 0.2$ eV, the relation $\tilde{U}_1(\pi) = U_1$ holds and hence: $a = U_1$ and $b = 0$. Thus, bearing in mind that the ANCP's under consideration exhibit a profoundly narrow NBMO band, $w \leq 0.4$ eV [2], the lowest-excitation band can be correctly reproduced by the expression

$$E_1'(\omega) = 4\left[J - \frac{2\beta^2}{\tilde{U}_0 + 2J\cos\omega}\right]\sin^2(\omega/2), \tag{4.7}$$

where the renormalized Hubbard parameter $\tilde{U}_0 = U_0 - U_1$ has been introduced. As it is known an energy dispersion relation of the form (4.7) pertains to a magnon (spin-wave) collective excitation, exhibiting the characteristic ω^2-dependence for small values of ω [16]. Eq. (4.7) reveals that the long-range Coulomb interaction brings about an enhancement of the kinetic exchange term [10, 11] in comparison to the Hubbard case $U_1 = 0$

$$J_{\text{kin}} = -\frac{2\beta^2}{\tilde{U}_0 + 2J\cos\omega} \tag{4.8}$$

given by

$$\Delta J_{\text{kin}} = J_{\text{kin}}^{\text{Hub}} \frac{U_1}{\tilde{U}_0 + 2J\cos\omega} = J_{\text{kin}}^{\text{Hub}} \frac{1}{\alpha - 1}, \tag{4.9}$$

where

$$J_{\text{kin}}^{\text{Hub}} = -\frac{2\beta^2}{U_0 + 2J\cos\omega} \tag{4.10}$$

and $\alpha = U_0/U_1$. The replacement of $(U_0 \pm 2J)/U_1$ by α in Eq. (4.9) is justified in view of the fact that J is at least a factor of 10 smaller than the on-site Coulomb repulsion U_0.

In summary, we would like to reiterate the main results of the presented study on the elementary spin excitations in ANCP's:

(i) Utilizing an extended Hubbard-type Hamiltonian, which incorporates both nearest-neighbour Coulomb repulsion terms U_1 and exchange interactions J, we have calculated numerically the energy-dispersion relation for the lowest (collective) spin excitation.

(ii) The calculations imply that the long-range Coulomb repulsion lowers the excitation band energy, which amounts to impairing the stability of the ferromagnetically aligned state towards spin inversion in the NBMO band.

(iii) A strikingly precise agreement has been achieved by fitting an analytical formula to the exact numerical results. The explicit expression for the energy dispersion of the lowest excitation band, see Eq. (4.7), reveals that the main impact of the long-range Coulomb repulsion may be thought of as a renormalization (screening) of the on-site Coulomb parameter U_0, leading to an enhancement of the kinetic exchange term, see Eq. (4.9). The established renormalization of the Hubbard parameter to $U = U_0 - U_1$ is consistent with the earlier results by Paldus et al. [17], who used a value of $U \simeq 5$ eV in their Hubbard model considerations.

(iv) The lowest excitation mode is found to represent a magnon (spin-wave), propagating through the one-dimensional crystal. The stability of the saturated magnetic state, with respect to the magnon, depends on the competition between the exchange interaction J and the kinetic exchange term (4.8) characterizing

the ANCP. This is reflected by the sign of the net Heisenberg exchange interaction $J^{\text{eff}} = J - J_{\text{kin}}$, see Eq. (4.8).

Acknowledgements. One of us (C.I.I.) is indebted to the Alexander-von-Humboldt Foundation for financial support during his stay at the Max-Planck-Institut für Strahlenchemie, Mülheim a.d. Ruhr, FRG.

References

1. Tyutyulkov N, Schuster P, Polansky OE (1983) Theor Chim Acta 63:291
2. Tyutyulkov N, Polansky OE, Schuster P, Karabunarliev S, Ivanov CI (1985) Theor Chim Acta 67:211
3. Dewar NJ (1969) The MO theory of organic chemistry. McGraw-Hill, New York
4. Klein DJ, Nelin CJ, Alexander S, Matsen FA (1982) J Chem Phys 77:3101
5. Ovchinnikov AA (1978) Theor Chim Acta 47:297
6. Koutecky J, Döhnert D, Wormer PES, Paldus J, Cizek J (1984) J Chem Phys 80:2244
7. Teki Y, Takui T, Itoh K (1983) J Am Chem Soc 105:3722
8. Durand Ph (1983) Phys Rev A28:3184; Maynau D, Durand Ph, Daudey JP, Malrieu JP (1983) Phys Rev A 28:3193
9. Coulson CA, Rushbrooke GS (1940) Proc Cambridge Philos Soc 36:193
10. Heitler W, London F (1927) Z Phys 44:455; Heisenberg W (1926) Z Phys 38:411; Heisenberg W (1928) Z Phys 49:619
11. Van Vleck JH (1932) Theory of electric and magnetic susceptibilities, chaps XI and XII. Oxford University Press, London, New York; Anderson FW (1963) In: Seitz F, Turnbull D (eds) Solid state physics, vol 14. Academic Press, New York, London, p 99
12. Ivanov CI, Olbrich G, Barentzen H, Polansky OE (1986) Phys Rev B (1986), in press
13. Hubbard J (1963) Proc R Soc London A 276:238
14. Hubbard J (1964) Proc R Soc London A 281:401
15. Tyutyulkov N, Karabunarliev S (1986) Int J Quantum Chem 29:1325
16. Herring CH, Kittel C (1951) Phys Rev 81:869
17. Paldus J, Čižek J, Hubač I (1974) Int J Quantum Chem Symp 8:293; Paldus J, Boyle MJ (1982) Int J Quantum Chem 22:1281